Appl Phys B
DOI 10.1007/s00340-010-3901-5

Applied Physics B
Lasers and Optics

Single-mode operation regime for 12-fold index-guiding quasicrystal optical fibers

H. Zhao · R. Proietti Zaccaria · P. Verma · J. Song · H. Sun

Received: 17 November 2009

Abstract We have studied the extent of the single-mode operation regime for high symmetric index-guiding quasicrystal fibers by analyzing the validity of the effective V parameter, which is used to determine the single-mode cutoff for photonic crystal fibers. We demonstrate that this parameter can also be applied, without any approximations, to a high symmetric 12-fold Stampfli quasicrystal made of silica. We explain this result in terms of both intrinsic-quasicrystal defect and photonic crystal constituent units. We also analyze the extent of the second-order mode operation to further confirm the cutoff between the single- and multimode operations.

1 Introduction

Index-guiding photonic crystal fibers (IGPCFs), as a new family of optical fibers, have been investigated with a great deal of interest in the recent years [1–7]. The structure of IGPCFs resembles that of conventional fibers, as it is composed of a central core of high refractive index surrounded by a low effective refractive index cladding, which in turn follows a two-dimensional photonic crystal geometry. Owing to the phenomenon of total internal reflection, light tends to propagate in the central core of the IGPCF, developing a *fiber behavior*. An alternative way to picture an IGPCF is to imagine a two-dimensional photonic crystal made by drilling holes in a dielectric and *removing* just one hole at the center. The hole-free area would correspond to the fiber core whereas the remaining structure would behave as the cladding. Among the reasons stimulating the research in the field of photonic crystal fibers (PCFs), which include IGPCFs and band-gap photonic crystal fibers, we can find the extremely useful properties of endlessly single-mode and flattened dispersion [8–11], besides their reduced spatial dimensions compared to the conventional analogous. The first characteristic allows for the use of a PCF as a single-mode transmission channel for a wide range of wavelengths (this wavelength range can even spread over a few micrometers in certain configurations), while the second characteristic guarantees the transmission of the signal for long distances due to the absence of any dispersion. A detailed review of the progress in the field of PCF can be found in [12].

There are a few different geometries that can be chosen to realize a PCF. Specifically, in terms of the Bravais lattice, only five configurations are possible. Some of them, for example, triangular [1] or square [13] like claddings, have already been investigated. Besides geometries with translational periodicity, structure showing only rotational and reflection symmetries can also be considered to develop a fiber-like device. In particular, the general group of quasicrystals can be considered for this purpose. Although many studies have been reported in relation to the optical properties of photonic quasicrystals [14–17], only little can

H. Zhao · R. Proietti Zaccaria · J. Song · H. Sun
State Key Laboratory on Integrated Opto-electronics, College of Electronic Science and Engineering, Jilin University, Changchun, 130023, People's Republic of China

R. Proietti Zaccaria (✉)
Italian Institute of Technology, IIT, Via Morego 30, 16163 Genova, Italy
e-mail: remo.proietti@iit.it

P. Verma
Department of Applied Physics, Osaka University, Yamadaoka 2-1, Suita, Osaka 565-0871, Japan

P. Verma
Department of Frontier Biosciences, Osaka University, Yamadaoka 2-1, Suita, Osaka 565-0871, Japan

Published online: 06 February 2010

be found that concerns their application in the fiber branch [18–20].

Optical properties of index-guiding fibers are usually defined by the so called V parameter. This quantity is commonly used to determine the single-mode operation regime of the fiber, as it provides the threshold between the single and the multimode operations. The most general definition of the V parameter, valid for standard fibers, is

$$V(\lambda) = \frac{2\pi a}{\lambda}\left(n_{\mathrm{co}}^2 - n_{\mathrm{cl}}^2\right)^{1/2} \tag{1}$$

where a is the core radius, and n_{co} and n_{cl} are the refractive indices of the core and the cladding, respectively. An extension of this formula to the PCF was defined in terms of an *effective* V parameter as [6]

$$V_{\mathrm{eff}}(\lambda) = \frac{2\pi a}{\lambda}\left(n_{\mathrm{co,eff}}^2 - n_{\mathrm{cl,eff}}^2\right)^{1/2}. \tag{2}$$

Here $n_{\mathrm{co,eff}}$ and $n_{\mathrm{cl,eff}}$ are the effective refractive indices of the fundamental mode when the central core is considered or missing in the structure, respectively. They are analogous to n_{co} and n_{cl}, respectively, in (1). Since the geometrical configurations around the core can influence the value of refractive indices, it is necessary to consider them as the effective parameters. The core radius a is also the lattice constant in this case. While this formulation is valid for PCF, no justification of its usage for IGPQF can be found in the literature. In the present work we investigate this point and we will demonstrate that (2) can also be applied, without any approximation, to the 12-fold Stampfli quasicrystal fiber [17]. This result might sound quite surprising considering that quasicrystal structures do not posses any translational symmetry. In fact, this could imply a dependence of $n_{\mathrm{cl,eff}}$ on the dimensions of the quasicrystal itself which would be reflected on the V parameter. However, as we will show, the intrinsic characteristics of quasicrystal make it behave in a way other than what one would expect from the geometrical arrangement.

2 The structure

We have chosen the highly symmetric 12-fold Stampfli geometry as fiber cross-section, a sketch of which is shown in Fig. 1. This structure is made of square and triangular basic units, as discussed elsewhere [17]. The geometrical parameters used in these calculations are the lattice constant (distance between nearest air holes) $a = 2.4$ μm and $d/a = 0.65$, where d represents the diameter of the air hole. The material of the fiber is silica ($n = 1.444$).

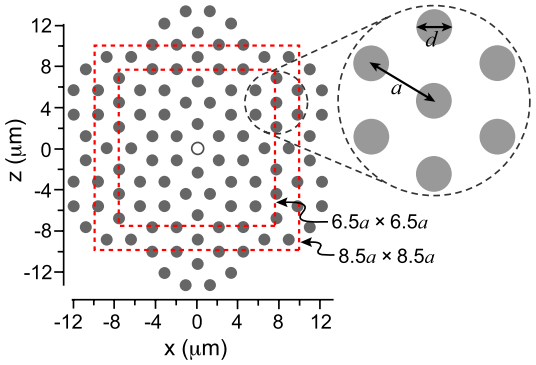

Fig. 1 Cross-sectional view of a 12-fold Stampfli quasicrystal fiber. The central hole (*empty circle*) is absent in the Stampfli IGPQC fiber. The quantities d and a are the hole radius and core radius (*pitch*), respectively. Two simulated domains with their size are shown by *the dashed squares*

2.1 Domain dependence

In order to carry on our investigation, we have evaluated the V parameters of both the Stampfli quasicrystal fiber and the standard hexagonal photonic crystal fiber, each for two different domains. This choice was motivated from the fact that these structures have exactly the same core (at a given pitch a and hole radius d) which in turn means that they would have very similar $n_{\mathrm{co,eff}}$. This reduces the complexity of the problem being only $n_{\mathrm{cl,eff}}$ the quantity to be analyzed. The numerical approach to evaluate V parameter makes use of the plane-wave expansion method in a frame of super-cell description. We have simulated a periodic structure where each unit cell was defined by the fiber of our interest. The distance between the cells was taken large enough so as to reduce any possible coupling between two adjacent cells as much as possible. Since the effective value of the V parameter includes the effective indices that depend on the extension of the fundamental mode as well as on the geometry and refractive index of the fiber itself, the value of the effective V parameter is in general approximate. In order to suppress the ambiguity in the value of the effective V parameter, we performed numerical simulations for different domains and at the same time assured the convergence in terms of the number of plane waves utilized in the calculation of the fiber modes. This gave us a convincing way to obtain accurate values of the effective V parameter. This method was utilized for both the 6-fold PCF and the 12-fold Stampfli IGPQF.

The two chosen domains for the present study are 6.5 square lattice constant ($6.5a \times 6.5a$) and 8.5 square lattice constant ($8.5a \times 8.5a$) in size, as shown by the areas within the two dashed squares marked in Fig. 1. With these calculations, we want to verify if there are any dependences of the V parameter on the domain area of the fiber for either hexagonal IGPCF or Stampfli IGPQF. Here, it should

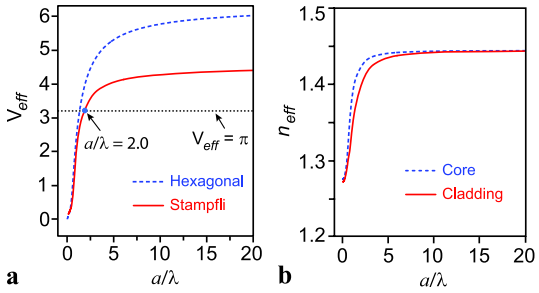

Fig. 2 (**a**) The effective V parameter for a hexagonal crystal fiber and a 12-fold Stampfli quasicrystal fiber. The calculations are performed for two different simulative domains (highlighted in Fig. 1) for $d/a = 0.65$. The results for both hexagonal IGPCF and Stampfli IGPQF for the two simulated domains are identical. Here *the dotted horizontal line* at $V_{\text{eff}} = \pi$ corresponds to the single-mode cutoff. In case of Stampfli IGPQF, the single-mode operation regime is given for $a/\lambda < 2$. (**b**) For the 12-fold Stampfli structure, the wavelength dependance of the effective refractive indices for both core and cladding

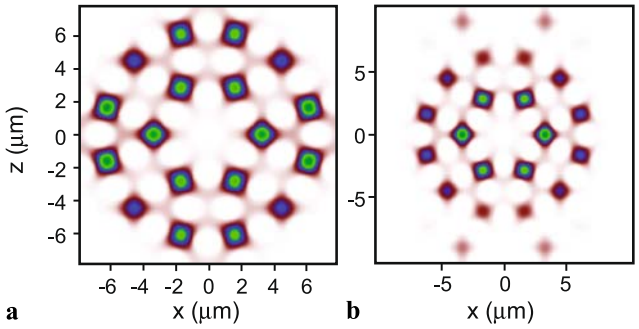

Fig. 3 Degenerative fundamental modes for the Stampfli IGPQF when the central hole is considered in the structure. The domain area in (**a**) is $6.5a \times 6.5a$, and in (**b**) is $8.5a \times 8.5a$. For both the domains $a/\lambda = 2.7$. The values of the refractive indices obtained from the simulation are exactly the same for the two cases ($V_{\text{eff}} = 1.417$). Four noticeable *fake* peaks in (**b**) originate from the artifact of the periodic boundary conditions

be noted that for a proper visualization of the V parameter, it is necessary that the domain size should at least be large enough to support the fundamental mode of the quasicrystal. The simulated results for the two chosen domain sizes are shown in Fig. 2(a). For a reference, the wavelength dependence of the effective refractive indices for both core and cladding, for the Stampfli structure, are shown in Fig. 2(b). As expected, the results for the hexagonal IGPCF are identical for the two simulated domains shown by the blue dashed curve in Fig. 2(a). This can easily be explained once we recall that IGPCFs are characterized by a translational periodicity, which implies Bloch behavior of the modes, which do not depend on the domain area. This mode, whose refractive index is exactly $n_{\text{cl,eff}}$, does not change even when we modify the domain area of the fiber. This, together with the obvious consideration that the fundamental mode of the structure without the central hole is also not affected by the domain area of the fiber, explains why no change in the V parameter of the hexagonal IGPCF can be noted when we move from $6.5a \times 6.5a$ to $8.5a \times 8.5a$ structure.

Now turning our focus to the Stampfli IGPQF, we might be driven to reach a wrong conclusion if we limit ourselves in considering the geometry of the quasicrystal. Indeed, as it is well known, quasicrystals do not posses any translational periodicity which implies no Bloch functions in the system are possible. This means that each mode is formed by isolated hot spots (corresponding to the peculiar hot spots of the quasicrystal) with an overall configuration that has to respect only the rotational and mirror symmetries of the structure. Moreover, because the number and distribution of hot spots change once we modify the domain area of the fiber, we could expect different fundamental modes for different dimensions. However, this is not what we find when we look at Fig. 2. Indeed, we see that the V parameters for the two simulated domains of the Stampfli quasicrystal fiber overlap with each other, shown by the red solid curve in Fig. 2(a). Only two situations can lead to this result–one, changing the cross-dimensions of the structure modifies both $n_{\text{co,eff}}$ and $n_{\text{cl,eff}}$ of the fundamental mode in such a way that $\Delta = n^2_{\text{co,eff}} - n^2_{\text{cl,eff}}$ remains constant; and two, no change in either of the effective refractive indices occurs. Simple consideration of the fundamental mode of the quasicrystal, when the central hole is absent, tells us that the only possible scenario is the latter one. To confirm this hypothesis we have calculated, for two different domain areas, the fundamental mode for the Stampfli quasicrystal fiber when the central hole is considered in the structure. This is intended to identify the mode whose refractive index is $n_{\text{cl,eff}}$. The results are shown in Fig. 3.

The two modes appear very similar to each other, with hot spots configurations that respect the constrains of rotational and mirror symmetries of the Stampfli quasicrystal. One can notice four hot spots existing only in the $8.5a \times 8.5a$ geometry, which actually do not correspond to the quasicrystal but they are due to the periodic boundary conditions imposed on the system which can create *fake* cavities close to the boundaries. These fake peaks originate due to the supercell method that is used in the numerical calculations. It can be clearly seen from Fig. 3 that the center of the Stampfli structure behaves similar to a defect in a standard photonic crystal. The fundamental mode thus adopts the spatial distribution of a cavity mode confined around the defect. This is why by changing the domain area of the Stampfli quasicrystal no appreciable differences among the fundamental modes can be observed. This, in turn, means no change in the effective refractive index, leading to the unchanged value of the V parameter. Hence, similar to IGPCFs, even 12-fold Stampfli IGPQFs show a V parameter that is independent of the extension of the domain.

2.2 Mode energy

The next interesting point to understand is the relation between the energies of the modes of the quasicrystal fiber and the modes associated with its constituent parts (basic units). We have recently demonstrated [17] how the optical gaps of a quasicrystal are intimately related to the band gaps of some of its constituent parts arranged in a crystal-like configuration. Keeping in mind that the basic constituent parts of the Stampfli 12-fold quasicrystal are squares and triangles with side-lengths a, we have calculated the fundamental modes for IGPCFs with geometries based on both the square and the triangular units. Our calculations show the existence of modes at energies exactly the same as those of the Stampfli modes of Fig. 3. This perfect matching between the modes of IGPCFs and IGPQFs can be considered as the second hint supporting the validity of (2) for quasicrystal fibers. Moreover, by looking at Fig. 3, we can immediately notice how the field distribution shows resonant peaks only inside the square units. No peaks are ever found in the triangular units. To explain this result, we calculated the value of the effective refractive indices associated with the square and the triangular IGPCFs, which were found to be 1.419 and 1.406, respectively. The higher value of refractive index associated with the square IGPCF, together with the electromagnetic variational principle, explains the field distribution in Fig. 3.

2.3 Mode width

After confirming our results for the fundamental mode, we further went on with calculations for the second-order mode. For this, we calculated the effective area in which the second-order mode of a Stampfli quasicrystal fiber extends. These simulations were also done for the domain areas of $6.5a \times 6.5a$ and $8.5a \times 8.5a$. The simulation results for the second-order mode are shown by the black squares in Fig. 4, which are presented in terms of the normalized effective area [3, 4]

$$A^{(j)}_{\text{eff,norm}} = \frac{[\int |E^{(j)}(s)|^2\, ds]^2}{\int |E^{(j)}(s)|^4\, ds}\,\frac{1}{a^2}. \tag{3}$$

Here E represents the electric field associated with the light, j identifies the mode and the integration is performed over ds that represents infinitesimally small area segment orthogonal to the fiber axis. The red curve in Fig. 4 represents a best fitted curve to the simulation results. It can be noted that we have chosen this fitting to be exponential in the present work, however, we could also obtain identical curve even with a polynomial fitting. The overall mathematical form of the fitting curve is not clear at present, however, the numerical values obtained from the fitting do not depend on the mathematical form of the curve, as long as one can obtain

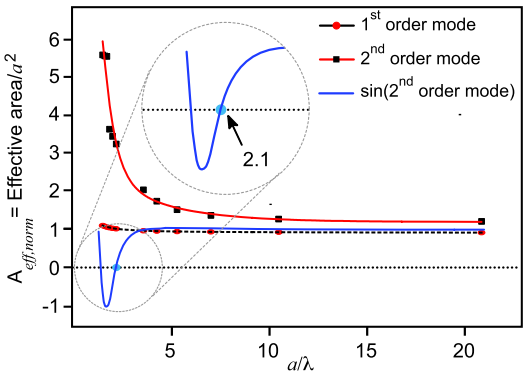

Fig. 4 Simulated normalized effective area for the first-order (*red circles*) and the second-order (*black squares*) modes for the Stampfli IGPQF when the central hole is considered in structure. The results are exactly the same for both $6.5a \times 6.5a$ and $8.5a \times 8.5a$ domain areas. *The black dashed* and *the red solid curves* are best fittings to the first- and the second-order modes, respectively. *The blue curve* represents the sin of the best fitting of the second-order mode, which shows the single-mode cutoff at $a/\lambda = 2.1$, an enlarged view of which is shown in the inset

a good fitting. We therefore note that, even though an exponential fitting may not be correct, it still gives us the best results within the wavelength range considered in the present study. For a comparison between the first- and the second-order modes, similar results for the first-order mode are also shown in Fig. 4 (red circles and black dashed curve), which shows that for smaller values of λ, the two modes tend to coincide. Confirming the predictions of Fig. 2, our calculations show substantially identical values for the two simulated domains.

A common way to estimate the cutoff for the single-mode in this formulation is to draw a tangent to the second-order mode at higher values of the wavelength and find out where this tangent meets the horizontal axis. However, due to the graphical construction, this method is strongly affected by numerical errors. Indeed, a fiber behaves in multi-mode fashion as long as the second-order mode remains confined to the core. When the second-order mode jumps out of the core, the fiber starts to behave in single-mode fashion. The value of wavelength at which the mode area for the second-order mode increases, indicates the threshold for the cut-off. One way to determine this value is to find the solution of

$$\sin\big[A_{\text{eff,norm}}(a/\lambda)\big] = 0. \tag{4}$$

In fact, we need a rapidly varying function that can respond to any sudden change. The sine function does this job efficiently, as it enhances small variations in any given function. We have therefore chosen the sine function in (4). As one can notice from the blue curve in Fig. 4, this function remains constant except around zero, where it shows rapid change, indicating the variation in the extension of the second-order mode. Thus, by solving (4), we find the single-mode cutoff at $a/\lambda = 2.1$, shown in the inset of Fig. 4. At

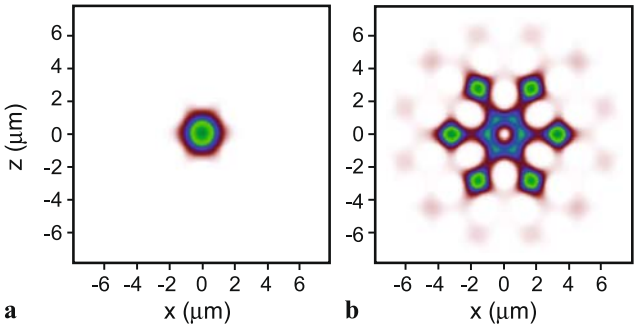

Fig. 5 The field distribution of the (**a**) first- and (**b**) second-order modes for a Stampfli IGPQF (no central hole) at $a/\lambda = 2.1$. At this value the second-order mode shows a cladding behavior. Both modes are degenerative

this value, $A_{\text{eff,norm}}$ for the fundamental mode is 0.95 which is more than three times smaller than the value for the corresponding second-order mode, which is 3.10. Such a big difference allows us to assume that the second-order mode is a cladding mode. In order to visualize and support our results, we calculated the first- and the second-order modes for a Stampfli IGPQF (without a hole at the center) at $a/\lambda = 2.1$. The results are shown in Fig. 5. As one can clearly see, the second-order mode at $a/\lambda = 2.1$ starts to show the cladding behavior. Hence, we conclude that the solution of (4) determines the single-mode cutoff ($a/\lambda = 2.1$) closer to the one obtained by examining the V parameter ($a/\lambda = 2.0$), which strongly supports the validity of (2) for IGPQCs.

Finally, we would like to note that there are possibilities of the fabrication [21] of non-periodic PCF, as for the case of the present work. One way of doing that for a quasicrystal fiber is to drill holes manually at a larger scale (for example, at millimeter scale), and then pull the fiber to make it thin and long.

3 Conclusions

In conclusion, we have demonstrated that the effective formula defining the V parameter for photonic crystal fibers can also be used, without any approximation, for the 12-fold Stampfli index-guiding quasicrystal fibers. This is explained by means of intrinsic defect nature of the quasicrystal and by means of the constituent parts description. Further, we have verified the value of the single-mode cutoff by calculating the area to which the second-order mode of the 12-fold Stampfli quasicrystal extends. The results match with the prediction coming from the V parameter calculation.

Acknowledgement The authors gratefully acknowledge support from NSF of China (NSFC) Grants No. 60525412 and No. 60677018.

References

1. J.C. Knight, T.A. Birks, P.St.J. Russell, D.M. Atkin, Opt. Lett. **21**, 1547 (1996)
2. J.C. Knight, T.A. Birks, P.St.J. Russell, D.M. Atkin, Opt. Lett. Errata **22**, 484 (1997)
3. T.M. Monro, D.J. Richardson, N.G.R. Broderick, P.J. Bennett, J. Lightwave Technol. **17**, 1093 (1999)
4. N.A. Mortensen, Opt. Exp. **10**, 341 (2002)
5. B.T. Kuhlmey, R.C. McPhedran, C.M. de Sterke, Opt. Lett. **27**, 1684 (2002)
6. N.A. Mortensen, J.R. Folkenberg, M.D. Nielsen, K.P. Hansen, Opt. Lett. **28**, 1879 (2003)
7. J.R. Folkenberg, N.A. Mortensen, K.P. Hansen, T.P. Hansen, H.R. Simonsen, C. Jakobsen, Opt. Lett. **28**, 1882 (2003)
8. T.A. Birks, J.C. Knight, P.St.J. Russell, Opt. Lett. **22**, 961 (1997)
9. A. Ferrando, E. Silvestre, J.J. Miret, P. Andres, Opt. Lett. **25**, 790 (2000)
10. W.H. Reeves, J.C. Knight, P.St.J. Russell, Opt. Exp. **10**, 609 (2002)
11. K. Saitoh, M. Koshiba, T. Hasegawa, E. Sasaoka, Opt. Exp. **11**, 843 (2003)
12. P.St.J. Russell, J. Lightwave Technol. **24**, 4729 (2006)
13. F. Poli, M. Foroni, M. Bottacini, M. Fuochi, N. Burani, L. Rosa, A. Cucinotta, S. Selleri, J. Opt. Soc. Am. A **22**, 1655 (2005)
14. Y.S. Chan, C.T. Chan, Z.Y. Liu, Phys. Rev. Lett. **80**, 956 (1998)
15. M.E. Zoorob, M.D.B. Charlton, G.J. Parker, J.J. Baumerg, M.C. Netti, Nature **404**, 740 (2000)
16. Y. Wang, X. Hu, X. Xu, B. Cheng, D. Zhang, Phys. Rev. B **68**, 165106 (2003)
17. H. Zhao, R. Proietti Zaccaria, J.F. Song, S. Kawata, H.B. Sun, Phys. Rev. B **79**, 115118 (2009)
18. J.S. Chiang, T.L. Wu, Opt. Commun. **258**, 170 (2006)
19. S. Kim, C.S. Kee, J. Lee, Opt. Exp. **15**, 13221 (2007)
20. S.M.A. Razzak, Y. Namihira, F. Begum, S. Kaijage, N.H. Hai, N. Zou, IEICE Trans. Electr. **E90-C**, 2141 (2007)
21. J. Canning, E. Buckley, K. Lyttikainen, T. Ryan, Opt. Commun. **205**, 95 (2002)